Caldesmon Inhibits Nonmuscle Cell Contractility and Interferes with the Formation of Focal Adhesions

David M. Helfman,* Esther T. Levy,†‡ Christine Berthier,*‡ Michael Shtutman,†‡ Daniel Riveline,†‡ Inna Grosheva,† Aurelie Lachish-Zalait,§ Michael Elbaum,§ and Alexander D. Bershadsky†‖

*Cold Spring Harbor Laboratory, Cold Spring Harbor, New York 11724; and Departments of †Molecular Cell Biology and §Materials and Interfaces, The Weizmann Institute of Science, Rehovot 76100, Israel

Caldesmon is known to inhibit the ATPase activity of actomyosin in a Ca^{2+}–calmodulin-regulated manner. Although a nonmuscle isoform of caldesmon is widely expressed, its functional role has not yet been elucidated. We studied the effects of nonmuscle caldesmon on cellular contractility, actin cytoskeletal organization, and the formation of focal adhesions in fibroblasts. Transient transfection of nonmuscle caldesmon prevents myosin II-dependent cell contractility and induces a decrease in the number and size of tyrosine-phosphorylated focal adhesions. Expression of caldesmon interferes with Rho A-V14-mediated formation of focal adhesions and stress fibers as well as with formation of focal adhesions induced by microtubule disruption. This inhibitory effect depends on the actin- and myosin-binding regions of caldesmon, because a truncated variant lacking both of these regions is inactive. The effects of caldesmon are blocked by the ionophore A23187, thapsigargin, and membrane depolarization, presumably because of the ability of Ca^{2+}–calmodulin or Ca^{2+}–S100 proteins to antagonize the inhibitory function of caldesmon on actomyosin contraction. These results indicate a role for nonmuscle caldesmon in the physiological regulation of actomyosin contractility and adhesion-dependent signaling and further demonstrate the involvement of contractility in focal adhesion formation.

INTRODUCTION

The regulation of the interactions between actin filaments and myosin molecular motors is essential for many cellular functions, from muscle contraction to signal transduction (Tan *et al.*, 1992; Brzeska and Korn, 1996; Burridge and Chrzanowska-Wodnicka, 1996; Squire and Morris, 1998). In addition to actin and myosin, other actin filament-associated proteins play basic roles in the regulation of cellular contractility, and these components differ between striated and smooth muscle and nonmuscle systems. In vertebrate skeletal and cardiac muscle, tropomyosins, in association with the troponin complex, regulate the calcium-sensitive interactions of actin and myosin II (Tobacman, 1996; Squire and Morris, 1998). In contrast, smooth muscle (as well as nonmuscle) cells do not express the troponin complex, and regulation of contractility is mediated by at least two independent mechanisms involving myosin light chain phosphorylation and caldesmon.

‡ These authors contributed equally to this work.
‖ Corresponding author. E-mail address: libersha@weizmann. weizmann.ac.il.

The regulation of actomyosin activity in smooth muscle and nonmuscle cells by phosphorylation of the regulatory light chain of myosin II (MLC) has been extensively characterized (Tan *et al.*, 1992; Somlyo and Somlyo, 1994). Phosphorylation of MLC by Ca^{2+}-calmodulin activated myosin light chain kinase leads to an increase in actomyosin ATPase activity and triggers myosin II-driven motility in vitro. Recently the small GTPase Rho was established to be a key regulator of MLC phosphorylation. GTP-bound Rho activates an enzyme known as Rho-kinase, which phosphorylates the myosin-binding subunit of myosin light chain phosphatase, inactivating it and thereby preventing MLC dephosphorylation (Kimura *et al.*, 1996). As a result, Rho activation leads to an accumulation of the phosphorylated MLC and, subsequently, to the stimulation of actomyosin ATPase activity.

The second type of regulation of myosin II activity involves caldesmon. This protein has been studied mainly in smooth muscle cells. Caldesmon contains actin-, myosin-, tropomyosin-, and Ca^{2+}–calmodulin-binding domains and acts by blocking the interaction of actin with myosin, inhibiting actin-activated myosin ATPase activity (for review, see Huber, 1997; Chalovich *et al.*, 1998; Marston *et al.*, 1998).

non-muscle caldesmon

Figure 1. Functional domains of nonmuscle caldesmon and a truncated caldesmon variant. Putative functional domains of the nonmuscle caldesmon molecule were determined by alignment of the nonmuscle and smooth muscle caldesmon using Clustal View software (Higgins *et al.*, 1991). Tropomyosin-binding domains are shown as open bars; myosin-binding domains are shown as spotty bars (the larger square spots correspond to stronger binding); actin- and calmodulin-binding domains are indicated by vertically and obliquely hatched bars, respectively (the density of hatching corresponds to the strength of binding). The digits at the ends of the bars and inside the bars correspond to the numbers of amino acid residues on caldesmon. The numbers in brackets indicate the following references: [1], Yamashiro *et al.* (1995); [2], Wang *et al.* (1997); [3], Wang *et al.* (1996); [4], Wang and Chacko (1996); [5], Marston *et al.* (1994); [6], Mezgueldi *et al.* (1994); and [7], Zhuang *et al.* (1995).

Caldesmon has been shown to affect several processes dependent on the actin–myosin interaction, including the movement of actin filaments over myosin heads as shown by in vitro motility assays (Okagaki *et al.*, 1991; Haeberle *et al.*, 1992; Shirinsky *et al.*, 1992; Fraser and Marston, 1995; Wang *et al.*, 1997) and tension development in skinned smooth muscle fibers (Katsuyama *et al.*, 1992; Pfitzer *et al.*, 1993).

Although the majority of experimental data cited above were obtained using smooth muscle caldesmon, the properties of nonmuscle caldesmon should be quite similar (for review, see Matsumura and Yamashiro, 1993; Huber, 1997). Smooth muscle and nonmuscle caldesmon are expressed from a single gene via alternative RNA splicing (Hayashi *et al.*, 1992; Payne *et al.*, 1995), and except for the lack of a central "spacer" domain, nonmuscle caldesmon contains all the functionally important domains of the muscle-derived molecule (Figure 1). However, although studies in smooth muscle cells strongly suggest a role for caldesmon in the regulation of contractility, there is no direct evidence for such a role in nonmuscle cell systems (Huber, 1997). At the same time, it appears that changes in fibroblast contractility may proceed without any MLC phosphorylation changes (Obara *et al.*, 1995), suggesting that regulation of nonmuscle cell contractility may involve independent alternative mechanisms. Nonmuscle caldesmon would constitute a good candidate as an alternative regulator of actomyosin contractility.

Contractility of nonmuscle cells has recently been demonstrated to be intimately associated with adhesion and adhesion-dependent signaling. Focal adhesions are sites of contact between the cell surface and the extracellular matrix, where the associated actin stress fibers terminate. They comprise integrin-type extracellular matrix receptors and a number of intracellular structural and signaling proteins (for review, see Geiger *et al.*, 1995; Jockusch *et al.*, 1995; Burridge and Chrzanowska-Wodnicka, 1996; Ben-Ze'ev and Bershadsky, 1997). Rho was shown to be an essential mediator in pathways leading to formation of focal adhesions and to the associated focal adhesion–dependent signaling (Ridley and Hall, 1992; Hotchin and Hall, 1995; Clark *et al.*, 1998). Similarly to the Rho-mediated contractility regulation, the formation of focal adhesions has been shown to depend on Rho-kinase activation (Leung *et al.*, 1996; Amano *et al.*, 1997; Ishizaki *et al.*, 1997). Furthermore, chemical inhibitors of MLC phosphorylation have been shown to prevent Rho-induced formation of focal adhesions (Chrzanowska-Wodnicka and Burridge, 1996).

Another body of evidence documenting the role played by contractility in the regulation of focal adhesion signaling lies in studies using microtubule disruption as an inducer of cellular contractility. Microtubule disruption increases contractility in various cell types (Danowski, 1989; Lampidis *et al.*, 1992; Kolodney and Elson, 1995; Sheridan *et al.*, 1996; Canman and Bement, 1997). This process is accompanied by an increase of MLC phosphorylation (Kolodney and Elson, 1995) that can be a consequence of augmentation of Rho activity (Ren *et al.*, 1999). At the same time, the disruption of microtubules was shown to be sufficient to induce a rapid assembly of focal adhesions and downstream adhesion-dependent signaling (Bershadsky *et al.*, 1996; Enomoto, 1996; Liu *et al.*, 1998). Moreover, the effect of microtubule disruption on the focal adhesion formation and signaling can be prevented by the Rho inhibitor C3 botulinum toxin (Enomoto, 1996; Liu *et al.*, 1998), as well as by chemical inhibitors of MLC phosphorylation (Bershadsky *et al.*, 1996). Altogether, these results led us to propose that an increase in cell

contractility is an indispensable step in the activation of adhesion-dependent signaling and focal adhesion formation.

Thus, most studies investigating the regulation of nonmuscle cell contractility and its relationship to adhesion-dependent signaling have focused on the role of myosin light chain phosphorylation and its upstream regulators. We show here that expression of nonmuscle caldesmon in cultured human fibroblasts inhibits cell contractility, as well as the assembly of stress fibers and focal adhesions, in a Ca^{2+}-sensitive manner. Thus, nonmuscle caldesmon can control contractility in fibroblasts and consequently affect adhesion-dependent signaling. In addition, these data further demonstrate that stimulation of contractility is an indispensable step in adhesion-dependent signaling processes.

MATERIALS AND METHODS

Cells

The SV80 cell line, derived from simian virus (SV40)-transformed, but weakly tumorigenic, human fibroblasts (Kahn et al., 1983) was used in all the experiments. The cultures were maintained in Dulbecco's modified Eagle's medium supplemented with 10% bovine calf serum (Hyclone, Logan, UT). Subconfluent cultures were transfected and examined 24–36 h later with or without incubation in serum-free medium and drug treatment.

cDNA Constructs and Transfections

cDNA clones encoding constitutively active Rho A-V14 kindly provided by Dr. A. Hall (University College, London, United Kingdom) and nonmuscle rat caldesmon (Yamashiro et al., 1995), a gift from Dr. F. Matsumura (Rutgers University, Piscataway, NJ), were PCR amplified and cloned in-frame between the XbaI and BamHI sites in the pCGN expression vector with an N-terminal 16-aa hemagglutinin (HA) tag or an 11-aa vesicular stomatitis virus (VSV) tag (Tanaka and Herr, 1990; Temm-Grove et al., 1996). A scheme depicting the localization of actin-, myosin-, tropomyosin-, and Ca^{2+}–calmodulin-binding sites in the sequence of nonmuscle caldesmon is presented in Figure 1. The caldesmon deletion mutant CD445B ("truncated caldesmon") was used as a control. This mutant contains aa 237–445 of nonmuscle caldesmon but lacks the strong actin-binding sites, the high-affinity Ca^{2+}–calmodulin-binding sites, one of the tropomyosin-binding sites at the C terminus, as well as the myosin-binding domain at the N terminus (Figure 1). This deletion mutant of caldesmon was prepared by PCR using sense primer ACCTTCTAGAGAATTCATGACCCACAAAC (containing an XbaI site) and antisense primer ACCTGGATCCCTATTCCG-CAGGGACAGGAAGATC (containing a BamHI site) and subcloned into the pCGN expression vector as described above.

To visualize caldesmon in living cells a fusion construct comprising caldesmon and the green fluorescent protein (GFP) was created. GFP cloned into the pRK expression vector was kindly provided by Dr. B. Geiger (The Weizmann Institute of Science). To produce a GFP–caldesmon construct, GFP was amplified by PCR from the pRK vector using sense ACCTTCTAGAATGGTGAGCAAGGGC-GAGG and antisense ACCTACTAGTTTACTTGTACAGCTCGTC-CATG primers. The PCR product was digested by XbaI and SpeI and cloned into the pCGN vector bearing HA-tagged full-length or truncated CD445B caldesmon in the XbaI site. The GFP bearing pRK vector was also used as a control in transfection experiments and, in some cases, in cotransfection experiments with other constructs to visualize living, transfected cells.

Cells were transfected using Ca^{2+}-phosphate or LipofectAMINE (Life Technologies, Grand Island, NY). Five hours after transfection, the medium was changed, and the cells were incubated for an additional time interval in serum-containing or serum-free medium before experimental treatment or fixation.

Drug Treatment

Microtubule disruption and the consequent induction of focal adhesion formation was achieved with 10 μM nocodazole treatment of serum-starved cells for 30 min (Bershadsky et al., 1996). To inhibit Rho activity, C3 Botulinum toxin (10 μg/ml) was added to the culture in serum-containing medium and incubated overnight. H-7, a kinase inhibitor shown to suppress cell contractility (Volberg et al., 1994), was added to the medium for 30 min at a final concentration of 300 μM. To increase the intracellular Ca^{2+} concentration, cells were treated with the calcium ionophore A23187 (5 μM) or with the calcium ATPase inhibitor thapsigargin (1 μM). Alternatively, the intracellular Ca^{2+} concentration was increased by addition of 50–100 mM KCl to the culture medium, leading to depolarization of cell membrane and opening of voltage-gated Ca^{2+} channels (Chen et al., 1988; De Roos et al., 1997).

Nocodazole [methyl-(5-[2-thienylcarbonyl]-1H-benzimidazol-2-yl) carbamate] and H-7 [1-(5-isoquinolinylsulfonyl)-2-methylpiperazine] were obtained from Sigma (Rehovot, Israel). A23187 and thapsigargin were from Calbiochem (La Jolla, CA). Recombinant C3 toxin of Clostridium botulinum was purified as described (Dillon and Feig, 1995) following expression from a plasmid obtained from Dr. A. Hall (University College) and was kindly provided to us by Dr. Ronen Alon (The Weizmann Institute of Science).

Fluorescence Microscopy

Cells were simultaneously fixed and permeabilized in PBS containing 3% paraformaldehyde and 0.5% Triton X-100 for 2 min, postfixed in 3% paraformaldehyde for 20 min, and labeled using indirect immunofluorescence. Monoclonal antibody to paxillin was purchased from Transduction Laboratories (Lexington, KY), monoclonal anti-phosphotyrosine antibody (clone PT66), anti-VSV antibody (clone P5D4), FITC- and TRITC-labeled phalloidin from Sigma, and monoclonal anti-HA tag antibody (clone16B12) from Babco (Richmond, CA). Rabbit anti-phosphotyrosine antibody was kindly provided by Dr. I. Pecht (The Weizmann Institute of Science), and polyclonal anti-VSV-G antibody (Soldati and Perriard, 1991) was provided by Dr. J.-C. Perriard (Swiss Federal Institute of Technology, Honggerberg, Switzerland). FITC-, TRITC-, and Cy5-conjugated goat anti-mouse and anti-rabbit immunoglobulins were obtained from Jackson Laboratories (West Grove, PA).

Immunolabeling and photography were performed as described (Volberg et al., 1994). For the immunolabeling of cells double transfected with caldesmon and Rho A-V14, we used the constructs bearing different tags (VSV and HA) and labeled the cells with rabbit anti-VSV and mouse anti-HA antibodies, followed by goat anti-rabbit TRITC-conjugated and anti-mouse Cy5-conjugated antibodies. FITC-phalloidin was used to visualize F-actin in the same cells. For the visualization of phosphotyrosine in the cells transfected with GFP–caldesmon and VSV–Rho A-V14, we labeled the cells with mouse anti-VSV and rabbit anti-phosphotyrosine, followed by the same combination of secondary antibodies. The triple-stained specimens were examined by video microscopy using a Zeiss (Thornwood, NY) Axiovert fluorescence microscope with a Plan-Apochromat 100× numerical aperture 1.3 objective, charge-coupled device camera (Photometrics, Tucson, AZ) and the Priism and Delta-Vision software packages (Applied Precision, Issaquah, WA) on a Silicon Graphics computer (SGI, Mountain View, CA). We used FITC filters to visualize GFP fluorescence.

The Delta-Vision video microscopy system was also used for the observations of GFP–caldesmon dynamics in living cells. We used 35-mm plastic Petri dishes, in which circular holes were made and onto which number 1 glass coverslips were mounted with wax to allow high-resolution visualization. The cells were plated onto these chambers 5–7 h after the GFP–caldesmon transfection, and the
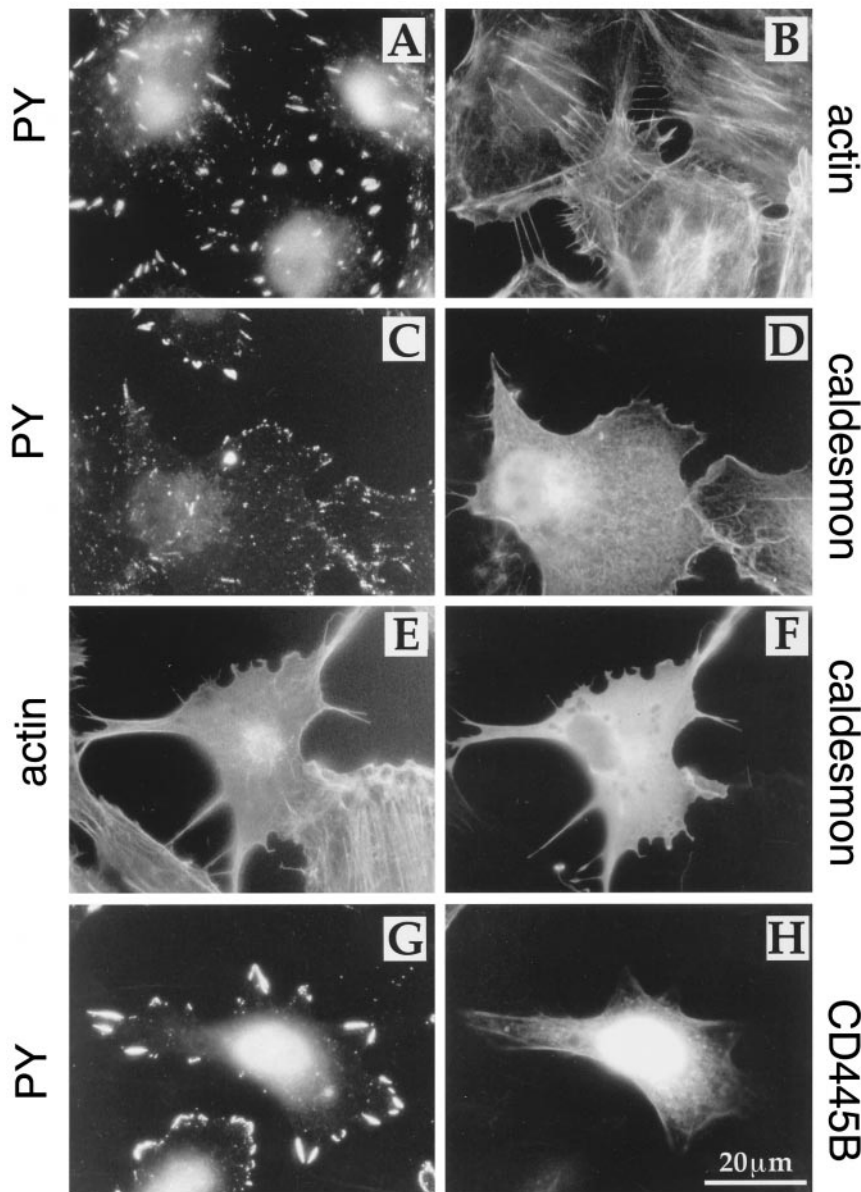
Figure 2. Effect of caldesmon overexpression on focal adhesions and the actin cytoskeleton of SV80 cells in serum-containing medium. (A and B) cells in control culture; (C–F) cells transfected with full-length caldesmon; (G and H) cells transfected with a truncated variant of caldesmon. Staining was performed with anti-phosphotyrosine (PY) antibody (A, C, and G), with FITC-phalloidin (B and E), and with anti-tag antibody to visualize transfected caldesmon (D, F, and H). (B, D, F, and H) Photographs of the same fields as in A, C, E, and G, respectively. Note that focal adhesions in cells expressing full-length caldesmon are much smaller than those in nontransfected cells or in cells expressing the truncated caldesmon (C compared with A and G). Stress fibers are abundant in nontransfected cells (B) but disappear in cells expressing full-length caldesmon (E and F). Some caldesmon-transfected cells show an increase in the formation of long processes (E and F).

observations were performed 16–20 h after plating. The objective was maintained at 37°C by a regulated electric heater while thermal contact through the immersion oil held the cells at the same temperature. The medium was buffered by 20 mM HEPES. Dynamics of GFP–caldesmon was registered by recording the fluorescent images every 10 min.

Quantitation of Focal Adhesions

To assess semiquantitatively the effects of different treatments and transfections on the formation and tyrosine phosphorylation of focal adhesions, we developed a simple classification system. The cells in each specimen were classified according to the prevailing size of their focal adhesions, as revealed by anti-phosphotyrosine labeling. The reference point in this classification was the predominant focal adhesion size in cells growing in serum-containing medium (Fig-

ures 2A and 3A). A majority of these cells have elongated focal adhesions of 3–5 μm length and ~1 μm in width. We defined the cells with prevalent focal adhesions of this size as belonging to the "medium" class. Cells in which the majority of focal adhesions had either greater width or length or were bigger in both dimensions formed the "large" class. Cells with prevalent small dot-like focal adhesions <1 μm in size were referred to as the "small" class. For each type of treatment, 100–200 randomly selected cells were scored.

Contractility Assays

The traction forces exerted by substrate-attached cells were assessed using the silicone–rubber substratum method (Harris *et al.*, 1980), modified according to Burton and Taylor (1997). Briefly, thin films of silicone rubber were prepared by vulcanizing the surface of a
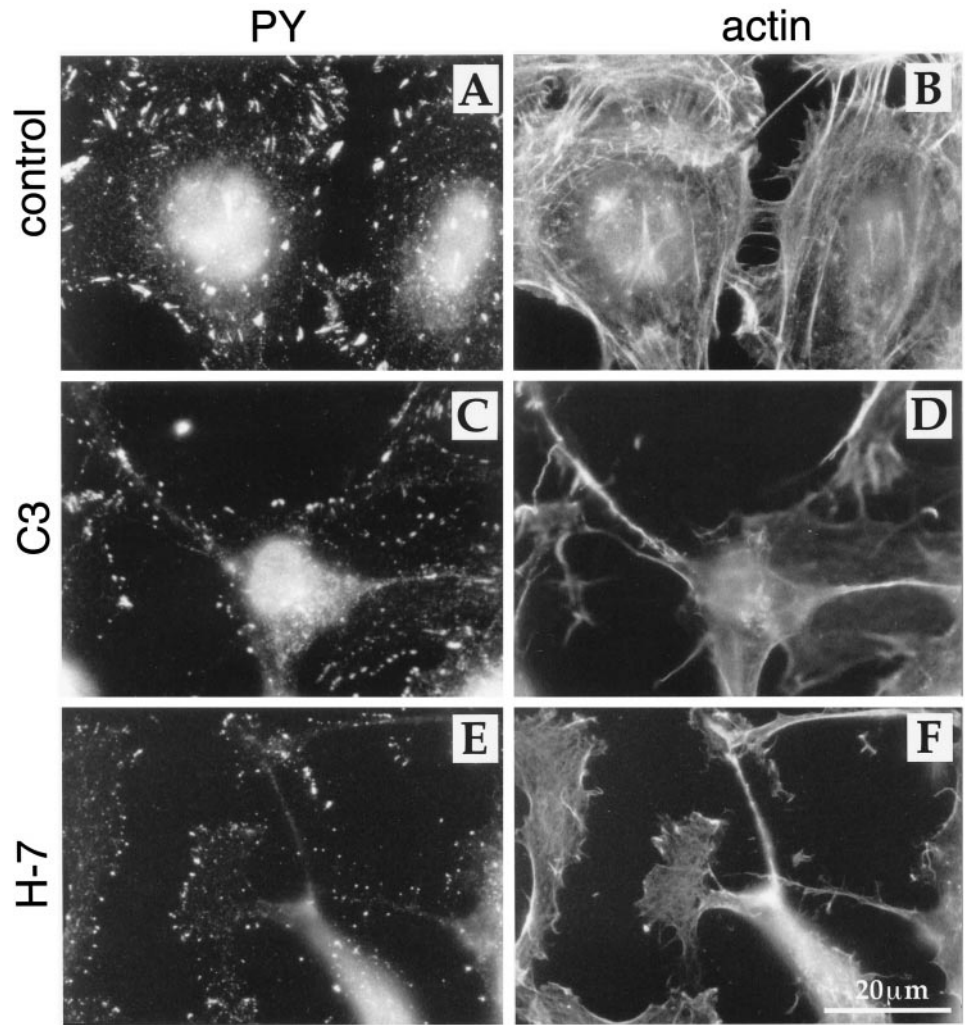
Figure 3. Botulinum C3 toxin and the H-7 serine/threonine kinase inhibitor induce alterations in cell morphology, focal adhesions, and the actin cytoskeleton similar to those induced by caldesmon transfection. (A and B) Control culture; (C and D) cells treated with C3 toxin; (E and F) cells treated with H-7. (A, C, and E) Staining with anti-phosphotyrosine antibody; (B, D, and F) staining with FITC-phalloidin of the same fields, respectively. Note significant decrease in the size of focal adhesions and disruption of actin stress fibers in cells treated with inhibitors. Note also that C3 toxin- and H-7-treated cells exhibit elongated cell processes (D and F).

layer of phenylmethyl polysiloxane, trimethyl terminated (710 fluid; Dow Corning, Midland, MI) with a Bunsen burner flame. Film compliance was increased by UV irradiation (3 h, at 1 cm from 15-W lamp; $\lambda = 312$ nm). Films were coated with fibronectin (F-1141, Sigma) by incubation with 10 μg/ml fibronectin solution in PBS for 24 h at 4°C before cell seeding. Cells were transfected with constructs encoding GFP–caldesmon, GFP–CD445B (truncated caldesmon), or GFP alone and plated on the films 10–20 h before the observations. The observations were performed using a Plan-Apochromat 40× numerical aperture 1.0 objective and phase-contrast optics.

To evaluate cell contractility, we also performed live recording of cell rounding after trypsin treatment (Symons and Mitchison, 1992). In these experiments the cells were cotransfected with GFP and caldesmon expression plasmids. Because the efficiency of cotransfection was estimated to be ~95%, as assayed by immunofluorescence labeling of cotransfected cells, we assumed that all GFP-fluorescent cells were also expressing caldesmon. The observations were performed using a Fluar 100×, numerical aperture 1.3 oil immersion objective and differential interference contrast optics. The serum-containing medium was changed to a serum-free medium 1 h before treatment. Standard 0.25% trypsin solution (Bio Labs, Jerusalem, Israel) was injected into the medium with a final dilution of 1:5. In these experiments the images were recorded by a digital charge-coupled device camera (iSight, Tirat haCarmel, Israel).

RESULTS

Effects of Caldesmon Overexpression on Cell Shape, the Actin Cytoskeleton, and Focal Adhesions

Subconfluent untreated SV80 cells in serum-containing medium exhibit a polygonal shape and form numerous elongated (dash-like) focal adhesions usually localized at the cell periphery. These focal adhesions were readily visualized by immunofluorescence labeling with an anti-phosphotyrosine antibody (Figure 2A), as well as with antibodies to vinculin or paxillin (see Figure 9). The actin cytoskeleton of SV80 fibroblasts, revealed by fluorochrome-conjugated phalloidin, showed actin filament bundles ("stress fibers") and a dense filamentous network localized in lamellipodia at the leading edges (Figure 2B).

Significant changes in cell shape, adhesion, and actin cytoskeletal organization were observed in subconfluent SV80
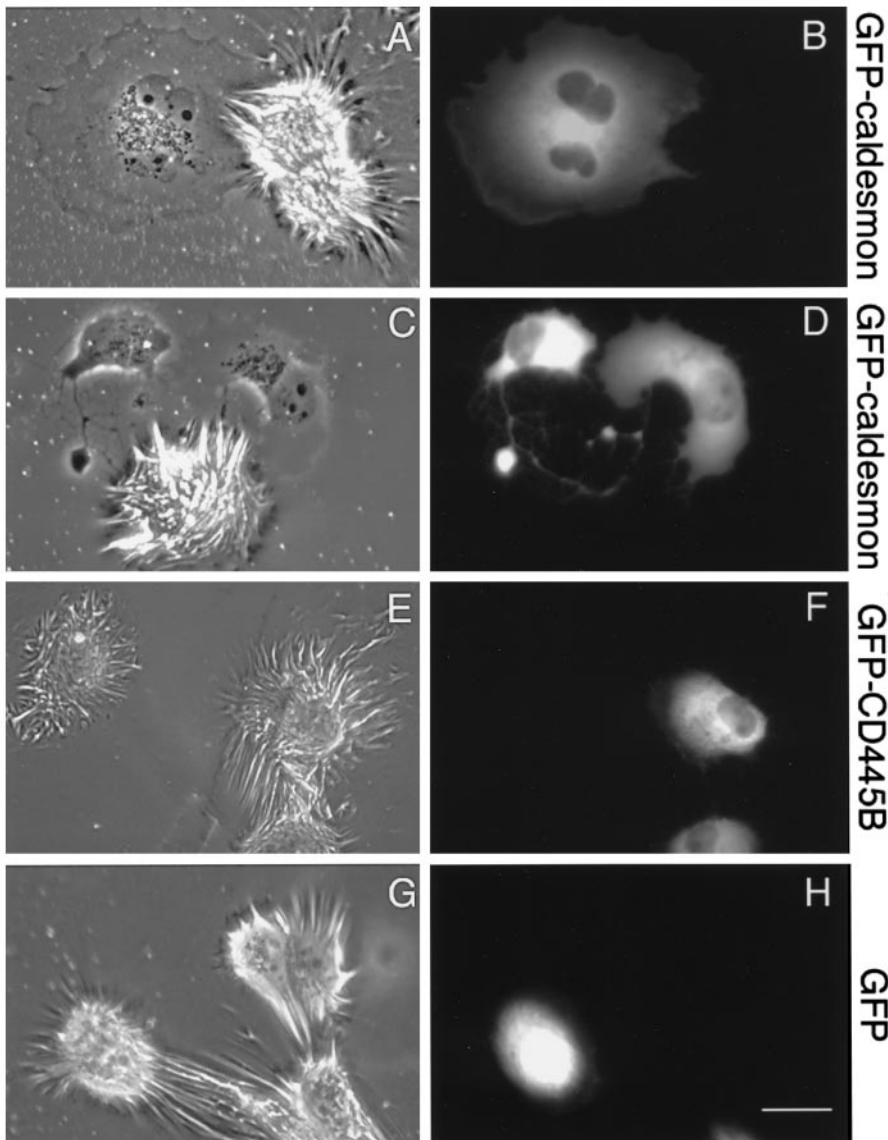
Figure 4. Caldesmon prevents development of traction forces in cells attached to an elastic silicone–rubber substrate. Cells were plated onto a fibronectin-coated silicone–rubber film 7 h after transfection with GFP-caldesmon (A–D), truncated caldesmon GFP–CD445B (E and F), or GFP alone (G and H) and photographed 20 h later. (A, C, E, and G) Phase-contrast images of substrate-attached cells and wrinkles they produce. (B, D, F, and H) GFP fluorescence images of the same fields showing that cells expressing full-length GFP–caldesmon cannot deform the substrate, whereas cells expressing truncated caldesmon, or GFP alone readily form wrinkles. Bar, 20 μm.

cells transfected with cDNA encoding full-length rat non-muscle caldesmon (Figure 2, C–F). Transfected cells acquired a characteristic morphology with augmented lamellipodia at the leading edge and elongated tails (Figure 2, D and F). Some cells with especially high levels of caldesmon expression became "arborized" because of the formation of long, slender, and sometimes branching cell processes (our unpublished results). Phalloidin staining of caldesmon-transfected cells revealed different stages of actin cytoskeleton disorganization. At 12–15 h after transfection, alterations in morphology were not yet very pronounced, and the transfected caldesmon in many cells was associated with normal actin-containing structures, including stress fibers. After 24–48 h of incubation, however, only a few caldesmon-transfected cells showed well-developed straight stress fibers, whereas the majority of cells exhibited altered, thin, and wavy stress fibers, to which the caldesmon

remained associated or demonstrated diffuse distribution of both actin and caldesmon (Figure 2, E and F). The truncated variant of caldesmon, CD445B, incorporated to some extent into stress fibers, although nuclear and diffuse cytoplasmic staining was more pronounced than in the case of full-length caldesmon (Figure 2H). Transfection with CD445B did not produce apparent changes in the actin cytoskeleton.

Anti-phosphotyrosine labeling showed that tyrosine phosphorylation in caldesmon-overexpressing cells was significantly lower than in control cells (Figure 2, C compared with A). Phosphotyrosine-containing focal adhesions in these cells were small, dot-like, and localized mainly at the edges of lamellipodial protrusions (Figure 2C). Transfection of cells with the truncated variant of caldesmon, CD445B, did not interfere with formation and tyrosine phosphorylation of focal adhesions (Figure 2G).
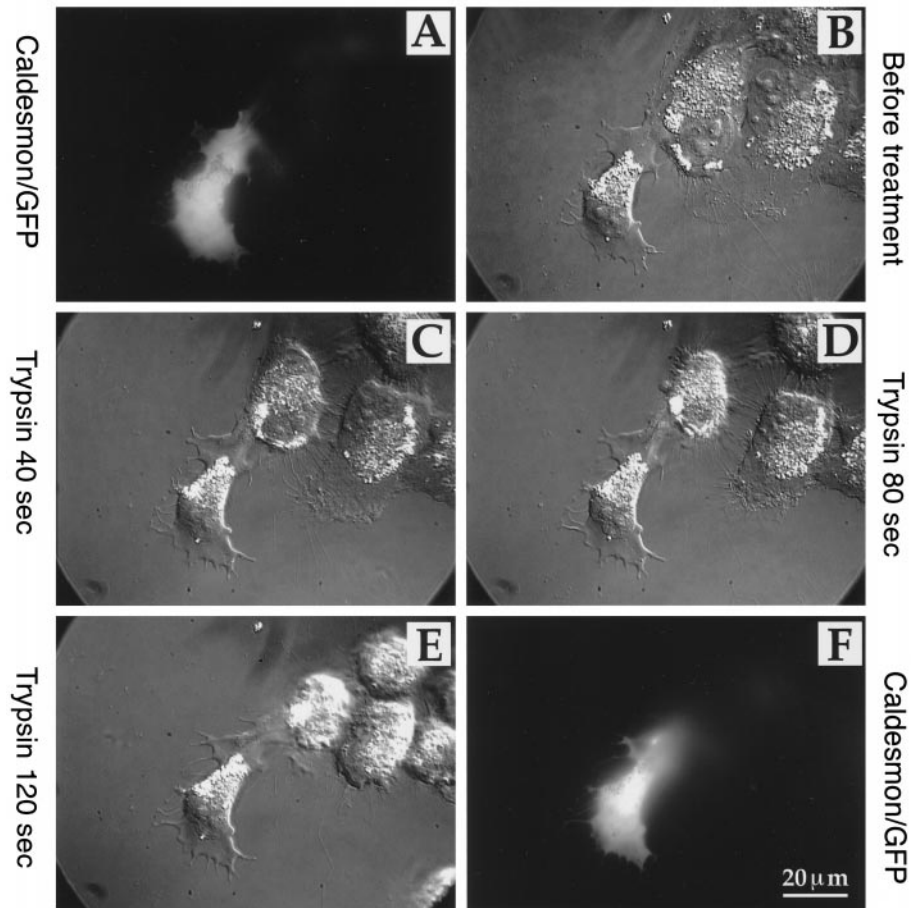
Figure 5. Caldesmon transfection prevents cell rounding induced by trypsin treatment. SV80 cells cotransfected with caldesmon and GFP were incubated in serum-free medium and treated with trypsin. Images were captured using fluorescence microscopy to identify transfected cells (A and F) and differential interference contrast optics to follow the changes in cell morphology induced by the treatment (B–E). (A and B) Culture before trypsin treatment; note transfected cell visualized by fluorescence in A. (C–E) Same field after 40, 80, and 120 s of trypsin treatment, respectively. (F) Fluorescence image corresponding to E. Note that the nontransfected cells retract and become round upon trypsin treatment, whereas the caldesmon-transfected cell does not significantly change shape (compare A and F).

The results of cell treatment with the protein kinase inhibitor H-7 and with the Rho inhibitor C3 botulinum toxin showed a striking similarity to the phenotypic effects of caldesmon overexpression (Figure 3). Treatment with these inhibitors led to an increase of protrusion activity, formation of elongated thin processes, and deterioration of stress fibers (Figure 3, D and F). The cells also failed to form large, dash-like focal adhesions, and labeling with anti-phosphotyrosine antibody revealed only small dot-like peripheral focal contacts (Figure 3, C and E compared with A).

Caldesmon Inhibits Cell Contractility

The contractility of caldesmon-transfected cells was assessed by examining the ability of substrate-attached cells to generate traction forces. This was analyzed in cells plated on elastic silicone rubber films after transfection with a construct encoding GFP–caldesmon (Figure 4). Formation of wrinkles on the silicone rubber film because of cell traction depends on the local compliance of the film. Because this parameter can vary from film to film and even from one area to another on the same film, we assessed the behavior of transfected cells only in the fields in which 100% of nontransfected neighboring cells exhibited apparent ability to form the wrinkles. Under these circumstances, the cells transfected with GFP–caldesmon demonstrated a se-

verely depressed ability to produce wrinkles, and ~90% of them did not induce wrinkling at all (Figure 4, A and C). Under the same conditions, ~80% of cells transfected with truncated caldesmon 445B were able to induce wrinkles (Figure 4E). The expression of GFP alone did not interfere with the ability of cells to generate wrinkles (Figure 4G).

Another assay used to demonstrate an inhibitory effect of caldesmon on cell contractility was trypsin-induced cell rounding. Trypsin treatment induces a rapid contraction in the majority of cell types, leading to complete cell rounding. Cell rounding depends on an actin–myosin interaction, as was shown on permeabilized cells (Sims *et al.*, 1992). Signals inducing rounding activate MLC phosphorylation in a Rho-dependent manner (Majumdar *et al.*, 1998). The rounding assay is convenient for analysis of actomyosin-driven cell contractility (Symons and Mitchison, 1992). As shown in Figure 5, the transfected cells did not round up after addition of trypsin, whereas neighboring, nontransfected cells became round in <2 min under these conditions (Figure 5, E and F compared with A and B). The rounding of cells transfected with GFP alone was not retarded when compared with the rounding of their nontransfected neighbors (our unpublished results). Caldesmon-transfected cells treated with 50 mM KCl for
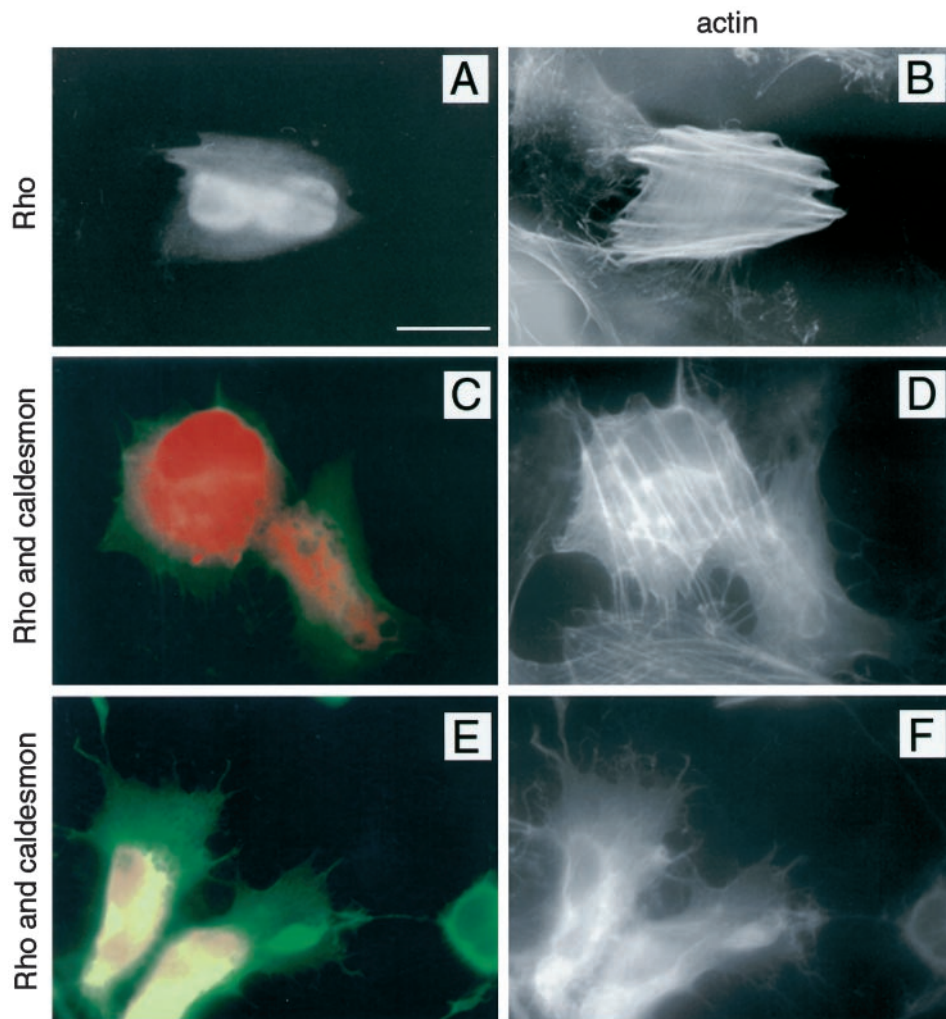
actin

Figure 6. Caldesmon interferes with Rho-induced enhancement of actin cable formation. (A and B) Cells transfected with activated Rho (Rho A-V14). Staining was performed with anti-tag antibody to visualize Rho A-V14 expression (A) and with phalloidin to visualize actin in the same cells (B). (C–F) Cells cotransfected with activated Rho and caldesmon. Triple staining was performed to visualize Rho, caldesmon, and F-actin in the same cultures. (C and E) Staining with antibodies to VSV and HA tag visualizing transfected Rho and caldesmon; intensities of staining are represented by pseudo colors: red corresponds to 100% Rho; green corresponds to 100% caldesmon; and intermediate orange–yellow colors correspond to different ratios between them. (D and F) Phalloidin staining of the same fields. Bar, 25 μm. Note that stress fibers in Rho-transfected cells (B) are much better developed than in neighboring (nontransfected) cells. The cells cotransfected with Rho and caldesmon assemble actin cables only if the level of Rho is much higher than the level of caldesmon (cell in the upper left part of C and D); if the level of caldesmon is comparable with that of Rho, formation of actin cables is blocked (cells in E and F).

30 min before trypsin addition demonstrated a rate of cell rounding similar to that of neighboring nontransfected cells (our unpublished results).

Caldesmon Prevents Formation of Focal Adhesions and Stress Fibers Induced by Activated Rho or by Microtubule Disruption

Transfection of SV80 cells with a cDNA encoding the constitutively activated Rho A-V14 induced dramatic changes in the organization of the actin cytoskeleton and focal adhesions, both in serum-free and in ordinary serum-containing medium. The transfected Rho A-V14 was diffusely distributed over the entire cytoplasm (Figures 6 and 7), as previously described (Adamson *et al.*, 1992). Phalloidin staining revealed very large bundles of actin in the Rho A-V14-transfected cells (Figure 6B).

To investigate the effects of caldesmon expression on the Rho-dependent formation of stress fibers and focal adhesions, cells were cotransfected with two different constructs, one encoding caldesmon, and the other encoding Rho A-V14. Double indirect immunofluorescence labeling of the cotransfected cells showed that 95% of the transfected cells expressed both proteins, although the level of expression of each varied between cells. Triple staining of tagged-Rho A-V14 and caldesmon together with F-actin allowed us to analyze the organization of the actin cytoskeleton with respect to the different ratios of Rho and caldesmon expression (Figure 6, C–F). These data showed that the expression of caldesmon could inhibit or even completely abolish the effect of Rho on cell morphology and the assembly of actin bundles. The cells expressing a high level of caldesmon did not form prominent actin stress fibers, even in the presence of comparable levels of Rho A-V14 (Figure 6, C–F). In addition, cells coexpressing Rho A-V14 and caldesmon often exhibited a shape similar to that of cells expressing caldesmon alone, with numerous lamellipodia and elongated processes (Figure 6, E and F). On the other hand, in the presence of low or intermediate levels of caldesmon, high expression of Rho still correlated with the display of stress fibers (Figure 6, C and D, left cell).

Cells doubly transfected with Rho A-V14 and caldesmon often showed small, dot-like focal adhesions (Figure
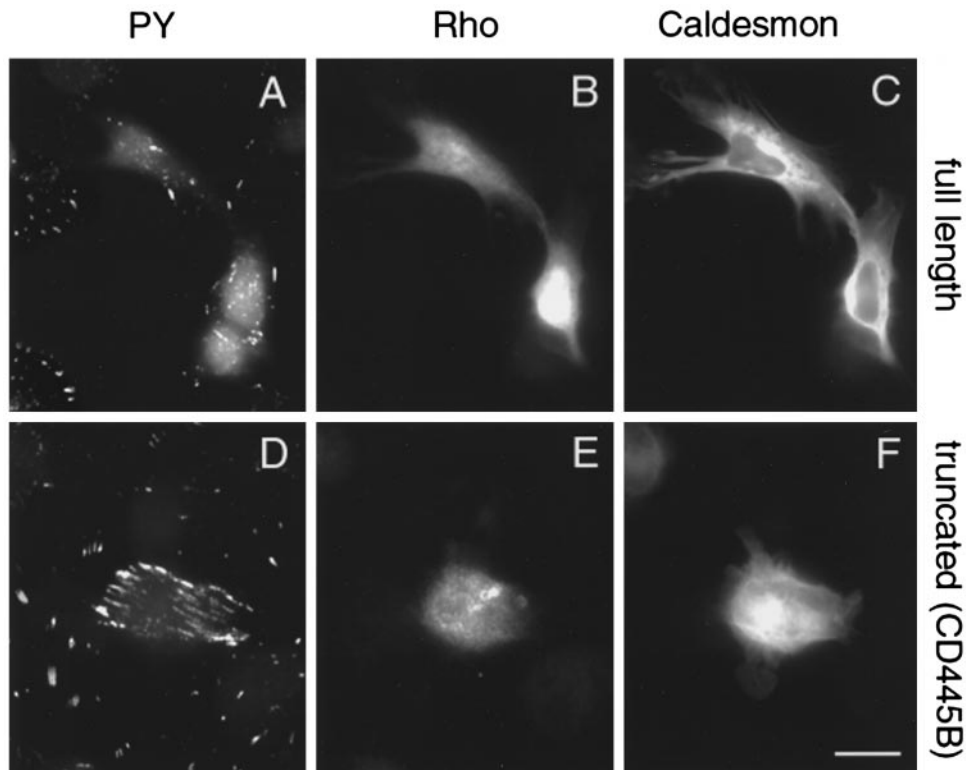
Figure 7. Effect of caldesmon expression on the Rho-induced formation of focal contacts. Triple labeling was performed to visualize phosphotyrosine (A and D), VSV-tagged Rho A-V14 (B and E), and GFP–caldesmon in the same cells. (A–C) Cells cotransfected with activated Rho and full-length GFP-caldesmon show predominantly dot-like focal adhesions. (D–F) Cells cotransfected with activated Rho and truncated GFP–CD445B caldesmon form large and intensely stained focal adhesions. Bar, 25 μm.

7A) typical of cells transfected with caldesmon alone (Figure 2C). Truncated CD445B caldesmon did not interfere with Rho-dependent stimulation of focal adhesion formation (Figure 7D). The effect of caldesmon and Rho A-V14 on the focal adhesions was quantified by classifying the cells according to the size of their focal adhesions after labeling with anti-phosphotyrosine antibody (see MATERIALS AND METHODS); the percentage of cells displaying each phenotype in the population of transfected cells was determined (Figure 8). These data showed that the cells expressing active Rho A-V14 all presented oversized focal adhesions when compared with mock-transfected cells (Figure 8, A and B). More interestingly, ~50% of the cells cotransfected with caldesmon and Rho exhibited tyrosine-phosphorylated focal adhesions that were smaller than those of cells transfected with Rho alone (Figure 8D). On the other hand, the fraction of cells with large focal adhesions was still higher in the population of doubly transfected cells when compared with the population of cells transfected with caldesmon alone (Figure 8, D compared with C). Thus, overexpression of full-length caldesmon efficiently inhibited formation of stress fibers and the phosphotyrosine-positive focal adhesions induced by activated Rho, but Rho also can partially suppress the effects of caldesmon.

We have previously shown that adhesion-dependent signaling, which includes formation of stress fibers and focal adhesions, is activated in serum-starved 3T3 fibroblasts by microtubule disruption (Bershadsky *et al.*, 1996). Microtubule disruption was shown to induce Rho activation (Ren *et al.*, 1999), MLC phosphorylation, and cell contraction (Danowski, 1989; Kolodney and Elson, 1995). We compared the effect of microtubule disruption on the formation of focal adhesions in control and caldesmon-transfected cells. SV80 cells were transfected with GFP–caldesmon, serum starved for 24 h, and treated with nocodazole for 30 min. Caldesmon-transfected cells, in contrast to the controls, did not form large phosphotyrosine- or paxillin-positive focal adhesions upon microtubule disruption (Figure 9, A and B). Scoring the cells according to the size of their focal adhesions showed that in serum-free medium, control or caldesmon-transfected SV80 cells formed mainly small focal adhesions (Figure 10, A and B). Addition of nocodazole induced the formation of numerous large focal adhesions in control cells, whereas caldesmon-expressing cells were much less affected (Figure 10, D compared with C). The difference between nocodazole-induced focal adhesion formation in mock-transfected and caldesmon-transfected cells was highly significant ($\chi^2 = 82$; $p \leq 0.001$). Thus, caldesmon expression, similar to chemical inhibitors that suppress cell contractility (Bershadsky *et al.*, 1996), can efficiently prevent the induction of focal adhesions by nocodazole.
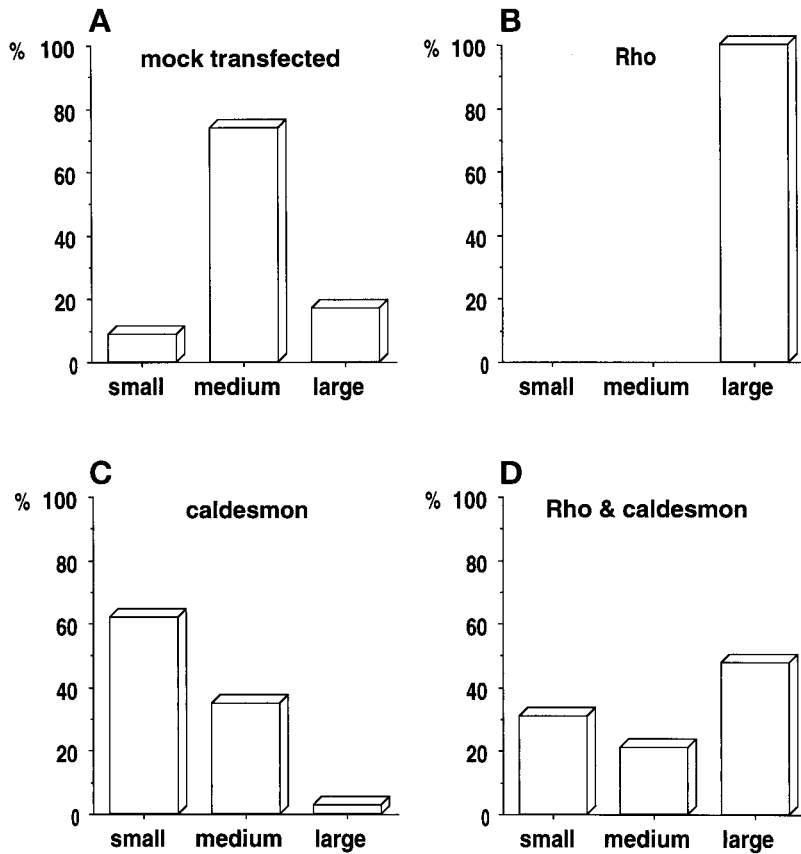
Figure 8. Quantification of effects of Rho and caldesmon on focal adhesions visualized by anti-phosphotyrosine staining. The percentage of cells having small, medium, and large focal adhesions was scored. Small refers to dot-like, nonelongated plaques; medium corresponds to typical dash-like adhesions in cultures of SV80 cells in serum-containing medium; and large denotes very large streak-like focal adhesions, typical of Rho-transfected cells. Note that Rho transfection induces formation of large focal adhesions in all cells (compare A and B), whereas caldesmon transfection efficiently decreases the percentage of cells with large focal adhesions, even in cells expressing activated Rho (C and D).

The Effects of Caldesmon on Focal Adhesions and Stress Fibers Are Ca²⁺ Sensitive

The inhibitory effect of caldesmon on the ATPase activity of actomyosin is reversible by calmodulin, calmodulin-like Ca^{2+}-binding protein, or S100 in the presence of Ca^{2+} (Marston *et al.*, 1998). Here we show that increased intracellular Ca^{2+} can reverse the inhibitory effects of transfected caldesmon on the assembly of stress fibers and focal adhesions. To investigate whether the effects of caldesmon in vivo are Ca^{2+} sensitive, we used several experimental procedures that increase the intracellular Ca^{2+} concentration via various mechanisms. These include treatment with the calcium ionophore A23187, with Ca^{2+}–ATPase inhibitor thapsigargin, which releases Ca^{2+} from intracellular stores (Treiman *et al.*, 1998), and with KCl, which induces membrane depolarization and opening of voltage-gated calcium channels.

All these treatments efficiently reversed the effects of overexpressed caldesmon. Caldesmon transfection, as described above, disorganized the actin cytoskeleton; as a result, GFP–caldesmon exhibited diffuse distribution with slightly increased intensity along a few wavy stress fiber remnants (Figure 11A). Video microscopic examination of GFP–caldesmon dynamics showed that thapsigargin (Figure 11) or KCl (our unpublished results) induced rapid recovery of the normal cytoskeleton structure with prominent caldesmon-containing stress fibers (Figure 11, B–F). This result demonstrates that caldesmon remains associated with the actin filament bundles even under conditions when its inhibitory effect on actin-myosin interaction is blocked by Ca^{2+}.

Treatment with the calcium-mobilizing compounds interfered with the inhibitory effect of caldesmon on focal adhesions. The percentage of cells with medium or large focal adhesions increased, whereas the percentage of cells with small focal adhesions decreased in caldesmon-transfected cells after KCl treatment (Figure 10, E and F). Increased intracellular Ca^{2+} abolished the inhibitory effect of caldesmon on formation of focal adhesions induced by microtubule disruption. When A23187 or thapsigargin was added to the medium before the nocodazole treatment, both transfected and nontransfected cells developed elongated mature focal adhesions of similar size (Figure 9, D and F). Formation of prominent focal adhesions in nocodazole-treated cells with elevated levels of intracellular Ca^{2+} was accompanied by the assembly of stress fibers to which GFP–caldesmon was localized (Figure 9, C and E). Collectively, these results demonstrate the calcium sensitivity of the inhibitory effect of caldesmon on focal adhesions and stress fibers.

DISCUSSION

Previous studies of contractility in nonmuscle cells have focused mainly on phosphorylation of the regulatory light chain of myosin. Here we demonstrate that regulation of contractility can occur through a mechanism involving non-muscle caldesmon. We have shown that both generation of

GFP-CALDESMON   PAXILLIN
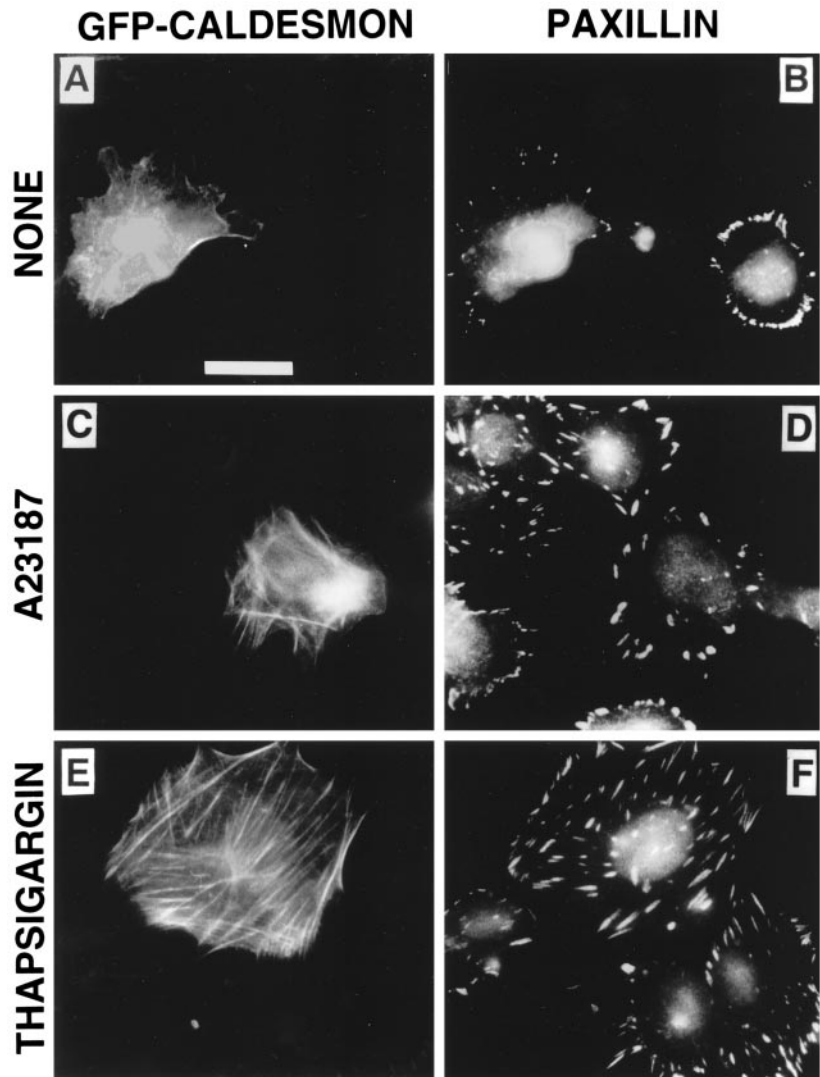
Figure 9. Effect of caldesmon on the stimulation of focal adhesion formation by nocodazole. Cells were transfected with GFP–caldesmon and serum starved for 24 h before nocodazole treatment. After treatment the cells were fixed and stained with mouse monoclonal antibodies against paxillin. (A, C, and E) GFP–caldesmon fluorescence is visualized; (B, D, and F) staining of the same fields with anti-paxillin antibody is presented. Bar, 20 μm. (A and B) Incubation with 10 μM nocodazole for 30 min induced formation of prominent focal adhesions in nontransfected cells (B, right cell) but not in the cells transfected with caldesmon (B, left cell). (C–F) Increased intracellular Ca^{2+} interferes with the inhibitory effect of caldesmon on focal adhesion and stress fiber formation. Five micromolar A23187 (C and D) or 1 μM thapsigargin (E and F) was added to the medium for 1 h before incubation with 10 μM nocodazole for an additional 30 min. Note that incubation with either A23187 or thapsigargin restores the ability of caldesmon-transfected cells to form large focal adhesions and stress fibers after nocodazole treatment (compare B with D and F). Caldesmon in the cells treated with calcium-mobilizing agents is localized to stress fibers (C and E).

traction forces by cells attached to flexible film and cell rounding after trypsin treatment were suppressed in the cells transfected with a construct encoding caldesmon. Overexpression of caldesmon was also able to inhibit contractility induced by microtubule disruption and expression of active Rho A-V14. Some caldesmon-transfected cells acquire a typical arborized shape with characteristic branching processes; this is likely to be a consequence of the inability of the cells with impaired contractility to retract their lamellipodial extensions and trailing edges ("tails") during locomotion. Comparable morphological changes were previously observed in cells microinjected with antibodies against myosin II (Honer et al., 1988) or treated with chemical inhibitors that block myosin II-driven contractility (Volberg et al., 1994). The apparent similarity between the morphological effects of these different agents strongly suggests that the changes in cell shape they induced are all related to their inhibitory effect on cell contractility.

Previous studies have localized endogenous caldesmon to actin filaments in cultured cells (Bretscher and Lynch, 1985;

Yamashiro-Matsumura and Matsumura, 1988; Hosoya et al., 1993). Our results with caldesmon overexpression are consistent with these observations. At early time points after transfection caldesmon is localized to stress fibers. Later, at 24–48 h after transfection, caldesmon exhibits its effects on stress fiber organization: straight, thick stress fibers gradually disappear and are replaced by less-defined wavy bundles of actin filaments, to which the exogenous caldesmon remains associated. It is interesting to note, however, that when the effect of caldesmon is blocked by elevated cytoplasmic Ca^{2+} levels (see below), the prominent stress fibers appear again, and exogenous caldesmon is still found associated to them. This result shows that the association of nonmuscle caldesmon with stress fibers is preserved even under conditions when its function is suppressed by Ca^{2+}–calmodulin. This is in agreement with studies in smooth muscle in which it was demonstrated that caldesmon remains associated with thin filaments in the presence of Ca^{2+} complex with calmodulin-like Ca^{2+}-binding protein (Marston et al., 1998).
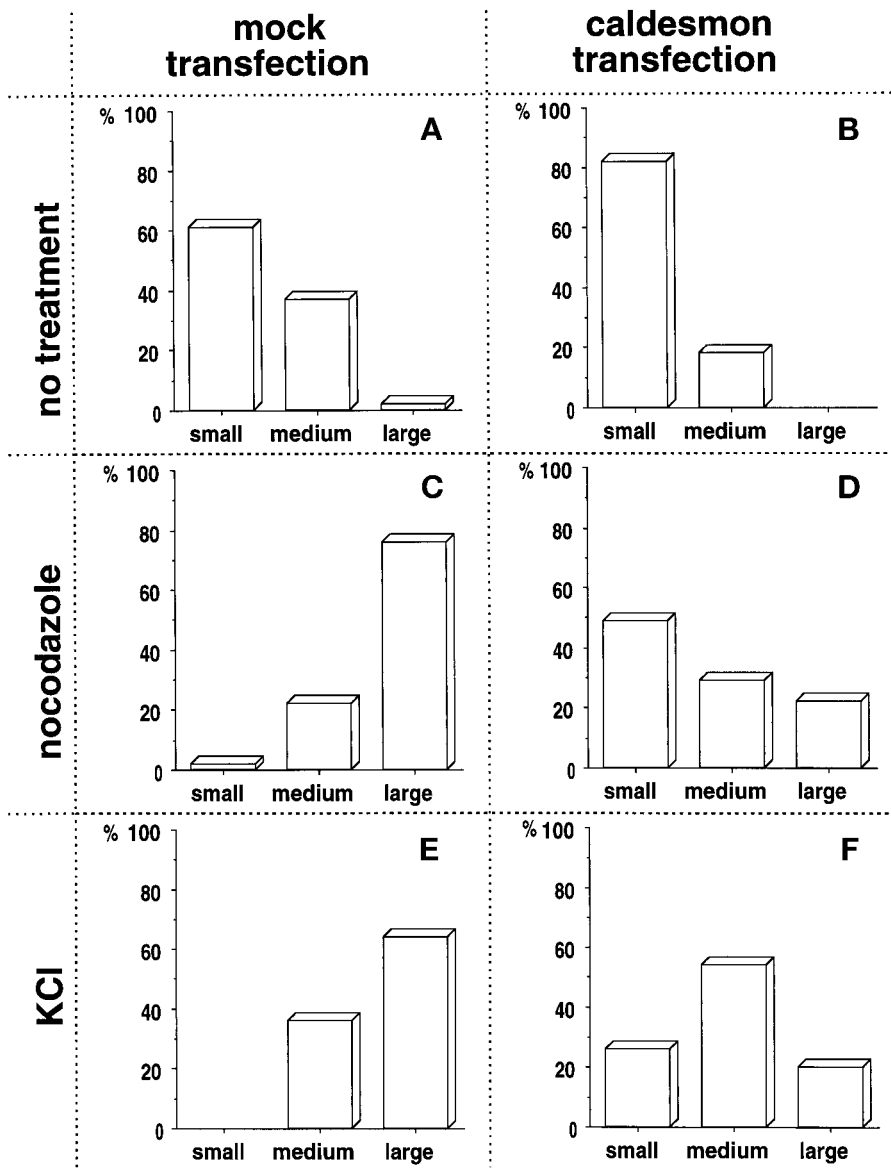
Figure 10. Quantification of the effects of caldesmon on the stimulation of focal adhesion formation by nocodazole and KCl treatment. Cells stained with anti-phosphotyrosine antibody and with anti-tag antibody visualizing transfected caldesmon were analyzed. The percentage of cells with small, medium, and large focal adhesions was scored. The diagram shows that transfection with caldesmon prevents stimulation of focal adhesion assembly by nocodazole, whereas stimulation by KCl is less severely affected.

We found that caldesmon-transfected cells, in the presence of serum, exhibit smaller focal adhesions with reduced levels of tyrosine-phosphorylated proteins compared with the nontransfected cells. These dot-like focal adhesions are usually concentrated at the leading edge and associated with poorly defined actin structures. This phenotype was essentially the same as that induced by chemical inhibitors of myosin-II-driven contractility or by Rho inactivation (Ridley and Hall, 1992; Volberg *et al.*, 1994; Bershadsky *et al.*, 1996; Chrzanowska-Wodnicka and Burridge, 1996; Pelham and Wang, 1997). Moreover, we have shown that caldesmon overexpression prevents the induction of focal adhesions and stress fibers by activated Rho or by microtubule disruption. Thus, inhibition of actomyosin contractility by caldesmon leads to the dissolution of preexisting focal adhesions and blocks their formation. These results, together with

experiments using inhibitors of MLC phosphorylation (Bershadsky *et al.*, 1996; Chrzanowska-Wodnicka and Burridge, 1996; Pelham and Wang, 1997), strongly suggest that the maintenance and assembly of focal adhesions depend on myosin II-driven contractility. It is worth noting that caldesmon has an advantage as an experimental tool over chemical inhibitors of myosin II function, because it is a natural and specific inhibitor of actomyosin contractility.

The specificity of the effects of nonmuscle caldesmon is supported by the following observations. First, these effects are Ca^{2+} sensitive, because they can be abrogated by increasing the cytoplasmic Ca^{2+} concentration. This characteristic is in agreement with the known calcium sensitivity of caldesmon effects in vitro mediated by Ca^{2+}-binding proteins such as calmodulin or S100 (Smith *et al.*, 1987; Pritchard and Marston, 1991; Marston *et al.*, 1998). Elevations of intra-
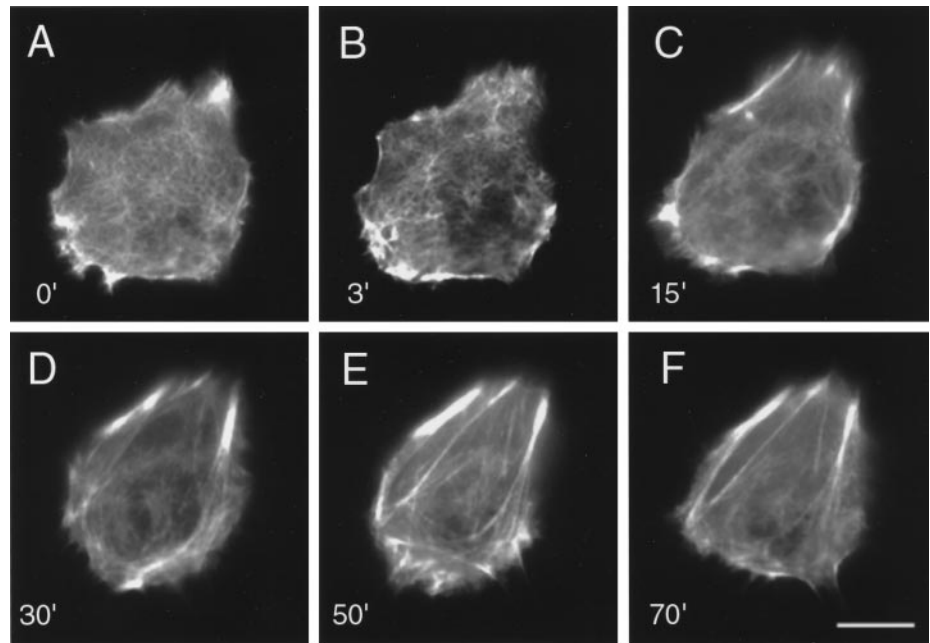
Figure 11. Reversal of the caldesmon effect by thapsigargin. GFP–caldesmon distribution in the transfected cell was visualized using video microscopy before (A) and 3 (B), 15 (C), 30 (D), 50 (E), and 70 (F) min after addition of thapsigargin. Note the absence of prominent stress fibers in the caldesmon-transfected cells and their recovery after thapsigargin treatment. Bar, 15 μm.

cellular Ca^{2+} could also be expected to lead to the stimulation of actomyosin ATPase through an increased phosphorylation of MLC by myosin light chain kinase (Tan *et al.*, 1992; Somlyo and Somlyo, 1994) and thereby indirectly counteract the effects of caldesmon on contractility. However, caldesmon still inhibits actomyosin ATPase and movement of actin filaments on smooth muscle myosin even if MLC is phosphorylated (Okagaki *et al.*, 1991; Shirinsky *et al.*, 1992). Thus we can attribute the observed restoration of actomyosin contractility to the effect of Ca^{2+} on caldesmon via Ca^{2+}-binding proteins.

Second, the truncated caldesmon CD445B mutant, lacking both a myosin-binding domain at the N terminus and a strong actin-binding site at the C terminus, does not exhibit any detectable biological activity in our experiments. In contrast, transfections with constructs containing either all the actin-binding sites of the molecule or truncated actin-binding domains together with intact myosin-binding domains at the N terminus are sufficient to produce phenotypic alterations similar to those induced by full-length caldesmon (our unpublished results). Detailed analysis of the in vivo functions of the different domains of nonmuscle caldesmon will require further work, but these observations clearly establish that the observed effects of caldesmon expression are due to its interactions with actin and myosin.

Thus, our results provide significant new evidence for the role of contractility in maintenance and formation of focal adhesions. The possible mechanisms underlying the relationship between contractility and the assembly of focal adhesions have been extensively discussed in the literature (Bershadsky *et al.*, 1996; Burridge and Chrzanowska-Wodnicka, 1996; Chrzanowska-Wodnicka and Burridge, 1996; Ben-Ze'ev and Bershadsky, 1997; Chicurel *et al.*, 1998; Elbaum *et al.*, 1998). A plausible suggestion is that the maintenance of focal adhesions depends on the tension developed by the actomyosin system, or, in other words, that focal adhesions belong to the class of "tensegrity" structures that preserve their integrity only under tension (Ingber, 1997). Involvement of the cytoskeletal tensegrity in integrin-dependent signaling was proposed by Ingber (1991, 1997) and Chicurel *et al.* (1998). In our model (Bershadsky *et al.*, 1996; Elbaum *et al.*, 1998) the nascent adhesive contacts in association with the actin cytoskeleton operate as tension-sensing devices converting mechanical signals into protein modification (such as tyrosine phosphorylation) and thus activate downstream intracellular pathways. The importance of tension for triggering adhesion-dependent signal transduction is supported by recent findings in which external forces applied to the cell–extracellular matrix adhesion sites, such as stretching of an elastic substrate (Hamasaki *et al.*, 1995; MacKenna *et al.*, 1998) or trapping of cell surface-attached beads (Choquet *et al.*, 1997; Schmidt *et al.*, 1998; Suter *et al.*, 1998), were shown to increase the strength of adhesion itself, the phosphorylation of focal adhesion proteins, and the progress of downstream signaling events. In addition, plating of cells on a very flexible substrate suppressed tension development and inhibited the formation and tyrosine phosphorylation of focal adhesions (Pelham and Wang, 1997). Collectively, these studies show that the tension-sensing molecular device, comprising focal adhesions and the actin cytoskeleton, has an important regulatory role in eukaryotic cells. This mechanism is under the control of several regulatory pathways, and we show here that caldesmon plays an important role in the regulation of this mechanism.

Caldesmon may be a target for a variety of signaling pathways that modulate its function and thereby its effect on cell contractility and adhesion-dependent signaling. Besides the calcium-sensitive regulation discussed above, it is known that caldesmon can be phosphorylated by serine/threonine kinases, including MAPK (Gerthoffer *et al.*, 1996), p34[cdc2] (Yamashiro *et al.*, 1991), p21-activated protein kinase

(Van Eyk *et al.*, 1998), and tyrosine kinases (McManus *et al.*, 1997). In some cases, this phosphorylation was shown to affect caldesmon function (for review, see Matsumura and Yamashiro, 1993). In the future, it will be of interest to determine whether caldesmon is a target for phosphorylation during activation of signaling pathways dependent on contractility, such as the Rho-dependent pathway.

Finally, tropomyosins are likely to play a significant role in the modulation of caldesmon function. Tropomyosins are natural partners of caldesmon in the regulation of actomyosin-based contractility and, indeed, can mediate the inhibitory effects of caldesmon on actomyosin (Horiuchi *et al.*, 1995; Hodgkinson *et al.*, 1997; Marston *et al.*, 1998). In nonmuscle cells, the diversity of tropomyosins is very large (Pittenger *et al.*, 1994; Gunning *et al.*, 1997; Lin *et al.*, 1997), and caldesmon specifically interacts with particular isoforms (Yamashiro-Matsumura and Matsumura, 1988; Novy *et al.*, 1993; Pittenger *et al.*, 1995), the biological significance of which remains unclear. Based on our results demonstrating the ability of caldesmon to regulate adhesion-dependent signaling, we suggest that specific tropomyosins could be important in maintaining the normal signaling function in the cell. This may provide a clue to explain the enigmatic correlation between the spectrum of tropomyosin isoforms and neoplastic transformation (Prasad *et al.*, 1993; Braverman *et al.*, 1996; Gimona *et al.*, 1996; Janssen and Mier, 1997).

Future studies will determine more precisely how caldesmon contributes to the regulation of nonmuscle cell contractility, how its function is regulated, and what role caldesmon plays in the signaling cascades associated with adhesion-mediated signal transduction.

ACKNOWLEDGMENTS

REFERENCES

Adamson, P., Paterson, H.F., and Hall, A. (1992). Intracellular localization of the p21rho proteins. J. Cell Biol. *119*, 617–627.

Amano, M., Chihara, K., Kimura, K., Fukata, Y., Nakamura, N., Matsuura, Y., and Kaibuchi, K. (1997). Formation of actin stress fibers and focal adhesions enhanced by Rho-kinase. Science. *275*, 1308–1311.

Ben-Ze'ev, A., and Bershadsky, A.D. (1997). The role of the cytoskeleton in adhesion-mediated signaling and gene expression. Adv. Mol. Cell Biol. *24*, 125–163.

Bershadsky, A., Chausovsky, A., Becker, E., Lyubimova, A., and Geiger, B. (1996). Involvement of microtubules in the control of adhesion-dependent signal transduction. Curr Biol. *6*, 1279–1289.

Braverman, R.H., Cooper, H.L., Lee, H.S., and Prasad, G.L. (1996). Antioncogenic effects of tropomyosin: isoform specificity and importance of protein coding sequences. Oncogene *13*, 537–545.

Bretscher, A., and Lynch, W. (1985). Identification and localization of immunoreactive forms of caldesmon in smooth and nonmuscle cells: a comparison with the distributions of tropomyosin and alpha-actinin. J. Cell Biol. *100*, 1656–1663.

Brzeska, H., and Korn, E.D. (1996). Regulation of class I and class II myosins by heavy chain phosphorylation. J. Biol. Chem. *271*, 16983–16986.

Burridge, K., and Chrzanowska-Wodnicka, M. (1996). Focal adhesions, contractility, and signaling. Annu. Rev. Cell Dev. Biol. *12*, 463–518.

Burton, K., and Taylor, D.L. (1997). Traction forces of cytokinesis measured with optically modified elastic substrata. Nature *385*, 450–454.

Canman, J.C., and Bement, W.M. (1997). Microtubules suppress actomyosin-based cortical flow in *Xenopus* oocytes. J. Cell Sci. *110*, 1907–1917.

Chalovich, J.M., Sen, A., Resetar, A., Leinweber, B., Fredricksen, R.S., Lu, F., and Chen, Y.D. (1998). Caldesmon: binding to actin and myosin and effects on elementary steps in the ATPase cycle. Acta Physiol. Scand. *164*, 427–435.

Chen, C.F., Corbley, M.J., Roberts, T.M., and Hess, P. (1988). Voltage-sensitive calcium channels in normal and transformed 3T3 fibroblasts. Science. *239*, 1024–1026.

Chicurel, M.E., Chen, C.S., and Ingber, D.E. (1998). Cellular control lies in the balance of forces. Curr. Opin. Cell Biol. *10*, 232–239.

Choquet, D., Felsenfeld, D.P., and Sheetz, M.P. (1997). Extracellular matrix rigidity causes strengthening of integrin-cytoskeleton linkages. Cell *88*, 39–48.

Chrzanowska-Wodnicka, M., and Burridge, K. (1996). Rho-stimulated contractility drives the formation of stress fibers and focal adhesions. J. Cell Biol. *133*, 1403–1415.

Clark, E.A., King, W.G., Brugge, J.S., Symons, M., and Hynes, R.O. (1998). Integrin-mediated signals regulated by members of the rho family of GTPases. J. Cell Biol. *142*, 573–586.

Danowski, B. (1989). Fibroblast contractility and actin organization are stimulated by microtubule inhibitors. J. Cell Sci. *93*, 255–266.

De Roos, A., Willems, P.H., van Zoelen, E.J., and Theuvenet, A.P. (1997). Synchronized Ca^{2+} signaling by intercellular propagation of Ca^{2+} action potentials in NRK fibroblasts. Am J Physiol. *273*, C1900–C1907.

Dillon, S.T., and Feig, L.A. (1995). Purification and assay of recombinant C3 transferase. Methods Enzymol. *256*, 174–184.

Elbaum, M., Chausovsky, A., Levy, E.T., Shtutman, M., and Bershadsky, A.D. (1998). Microtubule involvement in regulating cell contractility and adhesion-dependent signaling: a possible mechanism for polarization of cell motility. Biochem. Soc. Symp. *65*, 147–172.

Enomoto, T. (1996). Microtubule disruption induces the formation of actin stress fibers and focal adhesions in cultured cells: possible involvement of the rho signal cascade. Cell Struct. Funct. *21*, 317–326.

Fraser, I.D., and Marston, S.B. (1995). In vitro motility analysis of smooth muscle caldesmon control of actin-tropomyosin filament movement. J. Biol. Chem. *270*, 19688–19693.

Geiger, B., Yehuda-Levenberg, S., and Bershadsky, A.D. (1995). Molecular interactions in the submembrane plaque of cell-cell and cell-matrix adhesions. Acta Anat. *154*, 46–62.

Gerthoffer, W.T., Yamboliev, I.A., Shearer, M., Pohl, J., Haynes, R., Dang, S., Sato, K., and Sellers, J.R. (1996). Activation of MAP kinases and phosphorylation of caldesmon in canine colonic smooth muscle. J. Physiol. *495*, 597–609.

Gimona, M., Kazzaz, J.A., and Helfman, D.M. (1996). Forced expression of tropomyosin 2 or 3 in v-Ki-ras-transformed fibroblasts results in distinct phenotypic effects. Proc. Natl. Acad. Sci. USA *93*, 9618–9623.

Gunning, P., Weinberger, R., and Jeffrey, P. (1997). Actin and tropomyosin isoforms in morphogenesis. Anat. Embryol. *195*, 311–315.

Haeberle, J.R., Trybus, K.M., Hemric, M.E., and Warshaw, D.M. (1992). The effects of smooth muscle caldesmon on actin filament motility. J. Biol. Chem. *267*, 23001–23006.

Hamasaki, K., Mimura, T., Furuya, H., Morino, N., Yamazaki, T., Komuro, I., Yazaki, Y., and Nojima, Y. (1995). Stretching mesangial cells stimulates tyrosine phosphorylation of focal adhesion kinase pp125FAK. Biochem. Biophys. Res. Commun. *212*, 544–549.

Harris, A.K., Wild, P., and Stopak, D. (1980). Silicone rubber substrata: a new wrinkle in the study of cell locomotion. Science *208*, 177–179.

Hayashi, K., Yano, H., Hashida, T., Takeuchi, R., Takeda, O., Asada, K., Takahashi, E., Kato, I., and Sobue, K. (1992). Genomic structure of the human caldesmon gene. Proc. Natl. Acad. Sci. USA *89*, 12122–12126.

Higgins, D.G., Bleasby, A.J., and Fuchs, R. (1991). Clustal V: improved software for multiple sequence alignment. CABIOS *8*, 189–191.

Hodgkinson, J.L., Marston, S.B., Craig, R., Vibert, P., and Lehman, W. (1997). Three-dimensional image reconstruction of reconstituted smooth muscle thin filaments: effects of caldesmon. Biophys. J. *72*, 2398–2404.

Honer, B., Citi, S., Kendrick-Jones, J., and Jockusch, B.M. (1988). Modulation of cellular morphology and locomotory activity by antibodies against myosin. J. Cell Biol. *107*, 2181–2189.

Horiuchi, H.Y., Wang, Z., and Chacko, S. (1995). Inhibition of smooth muscle actomyosin ATPase by caldesmon is associated with caldesmon-induced conformational changes in tropomyosin bound to actin. Biochemistry *34*, 16815–16820.

Hosoya, N., Hosoya, H., Yamashiro, S., Mohri, H., and Matsumura, F. (1993). Localization of caldesmon and its dephosphorylation during cell division. J. Cell Biol. *121*, 1075–1082.

Hotchin, N.A., and Hall, A. (1995). The assembly of integrin adhesion complexes requires both extracellular matrix and intracellular rho/rac GTPases. J. Cell Biol. *131*, 1857–1865.

Huber, P.A. (1997). Caldesmon. Int. J. Biochem. Cell Biol. *29*, 1047–1051.

Ingber, D.E. (1991). Integrins as mechanochemical transducers. Curr. Opin. Cell. Biol. *3*, 841–848.

Ingber, D.E. (1997). Tensegrity: the architectural basis of cellular mechanotransduction. Annu. Rev. Physiol. *59*, 575–599.

Ishizaki, T., Naito, M., Fujisawa, K., Maekawa, M., Watanabe, N., Saito, Y., and Narumiya, S. (1997). p160ROCK, a Rho-associated coiled-coil forming protein kinase, works downstream of Rho and induces focal adhesions. FEBS Lett. *404*, 118–124.

Janssen, R.A., and Mier, J.W. (1997). Tropomyosin-2 cDNA lacking the 3′ untranslated region riboregulator induces growth inhibition of v-Ki-ras-transformed fibroblasts. Mol. Biol. Cell *8*, 897–908.

Jockusch, B.M., *et al.* (1995). The molecular architecture of focal adhesions. Annu. Rev. Cell Dev. Biol. *11*, 379–416.

Kahn, P., Topp, W.C., and Shin, S. (1983). Tumorigenicity of SV40-transformed human and monkey cells in immunodeficient mice. Virology *126*, 348–360.

Katsuyama, H., Wang, C.L., and Morgan, K.G. (1992). Regulation of vascular smooth muscle tone by caldesmon. J. Biol. Chem. *267*, 14555–14558.

Kimura, K., *et al.* (1996). Regulation of myosin phosphatase by Rho and Rho-associated kinase (Rho-kinase). Science *273*, 245–248.

Kolodney, M.S., and Elson, E.L. (1995). Contraction due to microtubule disruption is associated with increased phosphorylation of myosin regulatory light chain. Proc. Natl. Acad. Sci. USA *92*, 10252–10256.

Lampidis, T.J., Kolonias, D., Savaraj, N., and Rubin, R.W. (1992). Cardiostimulatory and antiarrhythmic activity of tubulin-binding agents. Proc. Natl. Acad. Sci. USA *89*, 1256–1260.

Leung, T., Chen, X.Q., Manser, E., and Lim, L. (1996). The p160 RhoA-binding kinase ROK alpha is a member of a kinase family and is involved in the reorganization of the cytoskeleton. Mol. Cell. Biol. *16*, 5313–5327.

Lin, J.J., Warren, K.S., Wamboldt, D.D., Wang, T., and Lin, J.L. (1997). Tropomyosin isoforms in nonmuscle cells. Int. Rev. Cytol. *170*, 1–38.

Liu, B.P., Chrzanowska-Wodnicka, M., and Burridge, K. (1998). Microtubule depolymerization induces stress fibers, focal adhesions, and DNA synthesis via the GTP-binding protein Rho. Cell Adhes. Commun. *5*, 249–255.

MacKenna, D.A., Dolfi, F., Vuori, K., and Ruoslahti, E. (1998). Extracellular signal-regulated kinase and c-Jun NH₂-terminal kinase activation by mechanical stretch is integrin-dependent and matrix-specific in rat cardiac fibroblasts. J. Clin. Invest. *101*, 301–310.

Majumdar, M., Seasholtz, T.M., Goldstein, D., de Lanerolle, P., and Brown, J.H. (1998). Requirement for Rho-mediated myosin light chain phosphorylation in thrombin-stimulated cell rounding and its dissociation from mitogenesis. J. Biol. Chem. *273*, 10099–10106.

Marston, S., *et al.* (1998). Structural interactions between actin, tropomyosin, caldesmon and calcium binding protein and the regulation of smooth muscle thin filaments. Acta Physiol. Scand. *164*, 401–414.

Marston, S.B., Fraser, I.D., Huber, P.A., Pritchard, K., Gusev, N.B., and Torok, K. (1994). Location of two contact sites between human smooth muscle caldesmon and Ca²⁺-calmodulin. J. Biol. Chem. *269*, 8134–8139.

Matsumura, F., and Yamashiro, S. (1993). Caldesmon. Curr. Opin. Cell Biol. *5*, 70–76.

McManus, M.J., Lingle, W.L., Salisbury, J.L., and Maihle, N.J. (1997). A transformation-associated complex involving tyrosine kinase signal adapter proteins and caldesmon links v-erbB signaling to actin stress fiber disassembly. Proc. Natl. Acad. Sci. USA. *94*, 11351–11356.

Mezgueldi, M., Derancourt, J., Calas, B., Kassab, R., and Fattoum, A. (1994). Precise identification of the regulatory F-actin- and calmodulin-binding sequences in the 10-kDa carboxy-terminal domain of caldesmon. J. Biol. Chem. *269*, 12824–12832.

Novy, R.E., Sellers, J.R., Liu, L.F., and Lin, J.J. (1993). In vitro functional characterization of bacterially expressed human fibroblast tropomyosin isoforms and their chimeric mutants. Cell Motil. Cytoskeleton. *26*, 248–261.

Obara, K., Nikcevic, G., Pestic, L., Nowak, G., Lorimer, D.D., Guerriero, V., Jr., Elson, E.L., Paul, R. J., and de Lanerolle, P. (1995). Fibroblast contractility without an increase in basal myosin light chain phosphorylation in wild-type cells and cells expressing the

catalytic domain of myosin light chain kinase. J. Biol. Chem. *270*, 18734–18737.

Okagaki, T., Higashi-Fujime, S., Ishikawa, R., Takano-Ohmuro, H., and Kohama, K. (1991). In vitro movement of actin filaments on gizzard smooth muscle myosin: requirement of phosphorylation of myosin light chain and effects of tropomyosin and caldesmon. J. Biochem. *109*, 858–866.

Payne, A.M., Yue, P., Pritchard, K., and Marston, S.B. (1995). Caldesmon mRNA splicing and isoform expression in mammalian smooth-muscle and nonmuscle tissues. Biochem. J. *305*, 445–450.

Pelham, R.J., Jr., and Wang, Y. (1997). Cell locomotion and focal adhesions are regulated by substrate flexibility. Proc. Natl. Acad. Sci. USA. *94*, 13661–13665.

Pfitzer, G., Zeugner, C., Troschka, M., and Chalovich, J.M. (1993). Caldesmon and a 20-kDa actin-binding fragment of caldesmon inhibit tension development in skinned gizzard muscle fiber bundles. Proc. Natl. Acad. Sci. USA. *90*, 5904–5908.

Pittenger, M.F., Kazzaz, J.A., and Helfman, D.M. (1994). Functional properties of nonmuscle tropomyosin isoforms. Curr. Opin. Cell Biol. *6*, 96–104.

Pittenger, M.F., Kistler, A., and Helfman, D.M. (1995). Alternatively spliced exons of the beta tropomyosin gene exhibit different affinities for F-actin and effects with nonmuscle caldesmon. J. Cell Sci. *108*, 3253–3265.

Prasad, G.L., Fuldner, R.A., and Cooper, H.L. (1993). Expression of transduced tropomyosin 1 cDNA suppresses neoplastic growth of cells transformed by the ras oncogene. Proc. Natl. Acad. Sci. USA. *90*, 7039–7043.

Pritchard, K., and Marston, S.B. (1991). Ca^{2+}-dependent regulation of vascular smooth-muscle caldesmon by S.100 and related smooth-muscle proteins. Biochem. J. *277*, 819–824.

Ren, X.D., Kiosses, W.B., and Schwartz, M.A. (1999). Regulation of the small GTP-binding protein Rho by cell adhesion and the cytoskeleton. EMBO J. *18*, 578–585.

Ridley, A.J., and Hall, A. (1992). The small GTP-binding protein rho regulates the assembly of focal adhesions and actin stress fibers in response to growth factors. Cell *70*, 389–399.

Schmidt, C., Pommerenke, H., Durr, F., Nebe, B., and Rychly, J. (1998). Mechanical stressing of integrin receptors induces enhanced tyrosine phosphorylation of cytoskeletally anchored proteins. J. Biol Chem. *273*, 5081–5085.

Sheridan, B.C., McIntyre, R.C., Jr., Meldrum, D.R., Cleveland, J.C., Jr., Agrafojo, J., Banerjee, A., Harken, A.H., and Fullerton, D.A. (1996). Microtubules regulate pulmonary vascular smooth muscle contraction. J. Surg. Res. *62*, 284–287.

Shirinsky, V.P., Biryukov, K.G., Hettasch, J.M., and Sellers, J.R. (1992). Inhibition of the relative movement of actin and myosin by caldesmon and calponin. J. Biol. Chem. *267*, 15886–15892.

Sims, J.R., Karp, S., and Ingber, D.E. (1992). Altering the cellular mechanical force balance results in integrated changes in cell, cytoskeletal and nuclear shape. J. Cell Sci. *103*, 1215–1222.

Smith, C.W., Pritchard, K., and Marston, S.B. (1987). The mechanism of Ca^{2+} regulation of vascular smooth muscle thin filaments by caldesmon and calmodulin. J. Biol. Chem. *262*, 116–122.

Soldati, T., and Perriard, J.C. (1991). Intracompartmental sorting of essential myosin light chains: molecular dissection and in vivo monitoring by epitope tagging. Cell *66*, 277–289.

Somlyo, A.P., and Somlyo, A.V. (1994). Signal transduction and regulation in smooth muscle. Nature *372*, 231–236 (erratum *372*, 812).

Squire, J.M., and Morris, E.P. (1998). A new look at thin filament regulation in vertebrate skeletal muscle. FASEB J. *12*, 761–771.

Suter, D.M., Errante, L.D., Belotserkovsky, V., and Forscher, P. (1998). The Ig superfamily cell adhesion molecule, apCAM, mediates growth cone steering by substrate-cytoskeletal coupling. J. Cell Biol. *141*, 227–240.

Symons, M.H., and Mitchison, T.J. (1992). A GTPase controls cell-substrate adhesion in *Xenopus* XTC fibroblasts. J. Cell Biol. *118*, 1235–1244.

Tan, J.L., Ravid, S., and Spudich, J.A. (1992). Control of nonmuscle myosins by phosphorylation. Annu. Rev. Biochem. *61*, 721–759.

Tanaka, M., and Herr, W. (1990). Differential transcriptional activation by Oct-1 and Oct-2: interdependent activation domains induce Oct-2 phosphorylation. Cell *60*, 375–386.

Temm-Grove, C.J., Guo, W., and Helfman, D.M. (1996). Low molecular weight rat fibroblast tropomyosin 5 (TM-5): cDNA cloning, actin-binding, localization, and coiled-coil interactions. Cell Motil. Cytoskeleton *33*, 223–240.

Tobacman, L.S. (1996). Thin filament-mediated regulation of cardiac contraction. Annu. Rev. Physiol. *58*, 447–481.

Treiman, M., Caspersen, C., and Christensen, S.B. (1998). A tool coming of age: thapsigargin as an inhibitor of sarco-endoplasmic reticulum Ca^{2+}-ATPases. Trends Pharmacol. Sci. *19*, 131–135.

Van Eyk, J.E., Arrell, D.K., Foster, D.B., Strauss, J.D., Heinonen, T.Y., Furmaniak-Kazmierczak, E., Cote, G.P., and Mak, A.S. (1998). Different molecular mechanisms for Rho family GTPase-dependent, Ca^{2+}-independent contraction of smooth muscle. J. Biol. Chem. *273*, 23433–23439.

Volberg, T., Geiger, B., Citi, S., and Bershadsky, A.D. (1994). Effect of protein kinase inhibitor H-7 on the contractility, integrity, and membrane anchorage of the microfilament system. Cell Motil. Cytoskeleton *29*, 321–338.

Wang, Z., and Chacko, S. (1996). Mutagenesis analysis of functionally important domains within the C-terminal end of smooth muscle caldesmon. J. Biol. Chem. *271*, 25707–25714.

Wang, Z., Horiuchi, K.Y., and Chacko, S. (1996). Characterization of the functional domains on the C-terminal region of caldesmon using full-length and mutant caldesmon molecules. J. Biol. Chem. *271*, 2234–2242.

Wang, Z., Jiang, H., Yang, Z.Q., and Chacko, S. (1997). Both N-terminal myosin-binding and C-terminal actin-binding sites on smooth muscle caldesmon are required for caldesmon-mediated inhibition of actin filament velocity. Proc. Natl. Acad. Sci. USA *94*, 11899–11891.

Yamashiro, S., Yamakita, Y., Hosoya, H., and Matsumura, F. (1991). Phosphorylation of nonmuscle caldesmon by p34cdc2 kinase during mitosis. Nature *349*, 169–172.

Yamashiro, S., Yamakita, Y., Yoshida, K., Takiguchi, K., and Matsumura, F. (1995). Characterization of the COOH terminus of nonmuscle caldesmon mutants lacking mitosis-specific phosphorylation sites. J. Biol. Chem. *270*, 4023–4030.

Yamashiro-Matsumura, S., and Matsumura, F. (1988). Characterization of 83-kilodalton nonmuscle caldesmon from cultured rat cells: stimulation of actin binding of nonmuscle tropomyosin and periodic localization along microfilaments like tropomyosin. J. Cell Biol. *106*, 1973–1983.

Zhuang, S., Wang, E., and Wang, C.L. (1995). Identification of the functionally relevant calmodulin binding site in smooth muscle caldesmon. J. Biol. Chem. *270*, 19964–19968.